Received May 28, 2021, accepted June 15, 2021, date of publication June 18, 2021, date of current version June 30, 2021.

Digital Object Identifier 10.1109/ACCESS.2021.3090473

Fault Evolution Monitoring of an In-Service Wind Turbine DFIG Using Windowed Scalogram Difference

ESTEFANIA ARTIGAO [1], JOSÉ MIGUEL BALLESTER-ARCE [2], MARÍA CARMEN BUESO [3], ANGEL MOLINA-GARCÍA [2], (Senior Member, IEEE), ANDRÉS HONRUBIA ESCRIBANO [1], AND EMILIO GÓMEZ LÁZARO [1], (Senior Member, IEEE)

[1] DIEEAC-ETSIIAB, Renewable Energy Research Institute, Universidad de Castilla-La Mancha, 02071 Albacete, Spain
[2] Department of Automatics, Electrical Engineering and Electronic Technology, Universidad Politécnica de Cartagena, 30202 Cartagena, Spain
[3] Department of Applied Mathematics and Statistics, Universidad Politécnica de Cartagena, 30202 Cartagena, Spain

Corresponding author: Estefania Artigao (estefania.artigao@uclm.es)

This work was supported in part by the Council of Communities of Castilla-La Mancha under Grant SBPLY/19/180501/000287, and in part by the European Union Fondo Europeo de Desarrollo Regional (FEDER).

ABSTRACT The rapid evolution of wind energy in reducing CO_2 emissions worldwide is undeniable, which is, in fact, expected to continue or even increase its impressive yearly capacity growth. In this regard, optimizing operations and maintenance of wind turbines (WTs) and farms is considered to be one of the options for reducing the levelized cost of electricity of wind energy. This can be achieved by developing innovative condition monitoring methods. To this end, the use of the windowed scalogram difference (WSD) algorithm, based on wavelets, is proposed as an alternative solution, combined with current signature analysis (CSA). The electric generator is one of the major contributors to WT failure rates and downtime, and doubly-fed induction generators (DFIGs) are the dominant technology in variable-speed WTs. In the present work, operational data on an in-service WT DFIG are analyzed over a period of eight months, in contrast to the majority of the studies in this field, which rely on laboratory or simulated data. The evolution of the fault, namely rotor mechanical asymmetry, at an early stage, is analyzed and quantified implementing WSD to the stator current signals, supported by the previous diagnosis achieved through CSA. The combination of CSA and WSD shows strong potential for diagnosing and tracking, respectively, incipient faults in in-service WT DFIGs.

INDEX TERMS Condition monitoring, current signature analysis, doubly-fed induction generator, wavelets, windowed scalogram difference, wind turbine.

I. INTRODUCTION

World wide climate change targets are set to reduce greenhouse gases (GHG) emissions towards a more sustainable world [1]. In Europe, the Strategic Energy Technology Plan [2] aims at reaching net zero CO_2 emissions by 2050. In this regard, renewable energies are playing, and will continue to play, a key role. Among these, wind energy is the most promising and mature of the different renewable energy sources [3]. In fact, despite the COVID-19 pandemic, 2020 was the best year in history for the global wind industry. With 93 GW of new installations, (of which 86.9 GW are onshore, 6.1 GW offshore) a global cumulative wind power capacity was brought up to 743 GW (of which 707.4 GW are onshore and 35.3 GW offshore) [4]. However, if the GHG emission targets are to be met, we need to be installing around 180 GW per year, and thus this new wind capacity record in 2020 fell short. Under this challenging scenario, it is crucial to reduce the levelized cost of electricity (LCOE) of wind energy, which is expected to be achieved through cost reduction from larger turbines, innovations in operations and maintenance (O&M), novel installations, and reduced investor risk [5]. The expectations to 2030 are 25% and 55% average LCOE reductions for onshore and offshore wind, respectively, compared to 2018 levels [5].

The associate editor coordinating the review of this manuscript and approving it for publication was Ton Duc Do.

Condition monitoring (CM) of wind turbines (WTs) is the key to reduce O&M costs while achieving higher availability [6]. The electric generator, together with the drive train and blades, is considered one of the most critical components within the WT [7]–[10]. Thus, considering the importance of optimizing O&M, highlighted by the fact that an increasing number of wind turbines (WTs) are reaching the end of their expected 20-year lifetime, the present work proposes a novel CM technique implemented on in-service WT generators. Specifically, we analyze doubly-fed induction generators (DFIGs), which are the dominant technology in variable-speed WTs [11], [12].

CM techniques for WT generators are mainly based on vibration or electrical measurements [13]. Lately, artificial intelligence applied to SCADA data has also recently proven successful in detecting different faults [14], although it is more commonly used for gearbox components. Combining different techniques for failure detection has also been explored, towards failure detection, such as SCADA data and vibrations [15] or joint current and vibration analyses [16]–[18]. On the other hand, whilst vibration-based techniques are limited to mechanical faults, electrically-based methods can detect both mechanical and electrical faults [19]. These methods include current, voltage, instantaneous power, and flux analyses [20], with current signature analysis (CSA) being recognized as the leading option [21]–[23]. Recent advances in CSA for WT generator applications were reviewed by [24], showing that the technique has been thoroughly studied. As can be concluded from this review, however, the studies are mostly limited to laboratory experiments and computer simulations. For example, rotor asymmetry [25], [26] and bearing faults [27] were analyzed and detected using test rigs, and inter-turn short circuit [28] and winding faults [29] were simulated using different computer models. CSA is also able to detect gearbox faults, as proven experimentally by [30]–[33] or simulated in [34], [35]. New signal processing approaches were proposed by [36] for generator bearing faults and by [37] for gearbox faults, again carried out in laboratory test rigs.

As can be deduced, data analyses of in-service WT DFIGs are rarely found in the scientific literature, where the immense majority of the published studies are carried out in laboratory benches or using computer simulated data. The analysis of operational data poses greater difficulties than laboratory or computer-based experiments, since these are unaffected by the grid and are not exposed to the actual unsteady load characteristics of WTs, extreme weather conditions or other external variables. Moreover, studies based on computer simulations or laboratory benches are performed under induced faults, that is, the faults are known. In this regard and to the best of our knowledge, only two research groups, besides the authors of the current work, have published such operational data analyses [38], [39]. Both works diagnose gearbox bearing fault through CSA, using the stator currents of in-service WT DFIGs.

The present paper aims to provide further analyses of WTs operating in the field with the ultimate goal of developing innovations in O&M. To this end, for the first time in the scientific literature, the windowed scalogram difference (WSD), a novel wavelet-based technique, is applied to the stator current measurements of an in-service WT DFIG over a period of eight months, being able to track and quantify the evolution of a potentially developing fault.

Further to this introduction, the paper is structured as follows: Section II explains the novel method proposed in the present work. Section III presents the data used for the analysis, including a summary of a previous study carried out by the authors of the present work. The results of implementing the novel method to the in-service WT DFIG are shown in Section IV. Finally, the conclusions drawn from the analysis are summarized in Section V.

II. WINDOWED SCALOGRAM DIFFERENCE

It is widely known that wavelet-based signal processing techniques consider both time and frequency domains simultaneously, allowing the decomposition of any signal into time scale components [40]. The Windowed Scalogram Difference (WSD) is a novel wavelet-based signal processing technique developed and introduced by Bolós *et al.* in [41]. This method was originally intended to measure the degree of non-periodicity of a time series, being more efficient than other approaches, such as the windowed Fourier transform (WFT), to that end. Indeed, the WSD can be considered as an alternative to another tool widely used in wavelet analysis: wavelet squared coherence (WSC). In some cases, the WSD is able to detect certain features that the WSC is unable to identify. Furthermore, the WSD gives greater flexibility in allowing the change of window size depending on the scale/horizon of interest [42]. The mathematical development behind the technique is presented as follows.

The scalogram of a time series, f, at a given scale, $s > 0$, is given by Equation 1 [43],

$$S(s) := \left(\int_{-\infty}^{\infty} |Wf(s,u)|^2 \, du \right)^{\frac{1}{2}}, \qquad (1)$$

The scalogram of f at s is then the $L2$–norm of $Wf(s,u)$ with respect to the time variable, u, and captures the energy of the continuous wavelet transform (CWT) of the time series f at this particular scale. Therefore, the scalogram allows the most representative frequencies (or scales) of a signal to be identified and detected, since such frequencies (or scales) contribute more to the total energy of the signal.

From Equation 1, it is possible to define the windowed scalogram for a specific time interval, $[t_0, t_1]$, as defined in Equation 2,

$$S_{[t_0,t_1]}(s) := \left(\int_{t_0}^{t_1} |Wf(s,u)|^2 \, du \right)^{\frac{1}{2}}, \qquad (2)$$

where $\tau = t_1 - t_0$ is defined as the time radius. Note that the windowed scalogram provides the relative importance of the different frequencies (or scales) around the given time point ($[t_0, t_1]$).

The *windowed scalogram* concept can be redefined by considering the function decomposition of the discrete wavelet transform (DWT) [44] and the use of the base 2 power scales [41] as per Equation 3,

$$WS_\tau(t,k) := \left(\int_{t-\tau}^{t+\tau} |Wf(u,2^k)|^2\,du\right)^{\frac{1}{2}}. \quad (3)$$

By considering finite time series $(t_0, \ldots, t_N)$ defined over a discrete set of times, border effects arise in the windowed scalogram for $t-\tau < t_0$ or $t+\tau > t_N$. In this case, Equation 3 can be redefined as Equation 4,

$$WS_\tau(t,k) := \frac{2\tau}{\Delta t}\left(\int_{t_\alpha}^{t_\beta} |Wf(u,2^k)|^2\,du\right)^{\frac{1}{2}}, \quad (4)$$

where $\Delta t = t_\beta - t_\alpha$, $t_\alpha := max(t-\tau, t_0)$ and $t_\beta := min(t+\tau, t_N)$. The factor $(2\tau/\Delta t)$ is variable, aimed at rectifying different border effects within the time interval.

Thus, the windowed scalogram difference (WSD) of two time series (f and g) with a time radius τ and centered at (t,k) is defined as Equation 5,

$$WSD_{\tau,r}(t,k) := \left(\int_{k-r}^{k+r}\left(\frac{WS_\tau(t,k) - WS'_\tau(t,k)}{WS_\tau(t,k)}\right)^2 dk\right)^{\frac{1}{2}}, \quad (5)$$

where $WS_\tau(t,k)$ and $WS'_\tau(t,k)$ are the corresponding *windowed scalograms* of the two time series (f and g), respectively, see Equation 3.

Furthermore, in order to avoid extreme (and thus misleading) results when the windowed scalogram takes values near zero, the WSD commutative version is more appropriate, calculated as Equation 6,

$$WSD_{\tau,r}(t,k) := \left(\int_{k-r}^{k+r}\left(\frac{WS_\tau(t,k) - WS'_\tau(t,k)}{WS_\tau(t,k)} + \frac{WS_\tau(t,k) - WS'_\tau(t,k)}{WS'_\tau(t,k)}\right)^2 dk\right)^{\frac{1}{2}}. \quad (6)$$

Finally, similarly to Equation 4, the WSD (Equations 5 and 6) can also be expressed as Equation 7, to reduce such WSD border effects,

$$WSD_{\tau,r}(t,k) := \frac{2r}{\Delta k}\left(\int_{k_\alpha}^{k_\beta}\left(\frac{WS_\tau(t,k) - WS'_\tau(t,k)}{WS_\tau(t,k)}\right)^2 dk\right)^{\frac{1}{2}}, \quad (7)$$

where $k_\alpha := max(k-r, 1+log_2(\Delta t))$, $k_\beta := min(k+r, log_2(N\Delta t/L))$, and L is the size of the original wavelet function.

Therefore, the WSD allows the similarity level between two times series (f and g) to be estimated for different finite time intervals and frequency (scale) intervals. According to [45], it is also worth highlighting that the great flexibility of the WSD arises from the possibility of shifting the length of time and scale windows. This WSD tool has been used in a wide variety of applications and scientific disciplines, such as image encryption [46], bio-medicine [47], meteorology [48], engineering [49] or robotics [50]. In this regard, to the best of the authors' knowledge, this is the first time that WSD has been implemented on current signals for condition monitoring of WT DFIGs.

III. BACKGROUND OF THE DFIG UNDER STUDY AND DATA USED

The DFIG under study comes from a 1.5 MW WT operating in an European wind farm. A previous study of the DFIG under analysis was presented in [51]. In the mentioned work, the authors achieved the diagnosis of the DFIG using CSA and validated it with advanced signal processing of vibration measurements. Figure 1 depicts a DFIG diagram indicating the stator- and rotor-side currents used for the analysis, and the characteristics of the signals used are presented in Table 1.

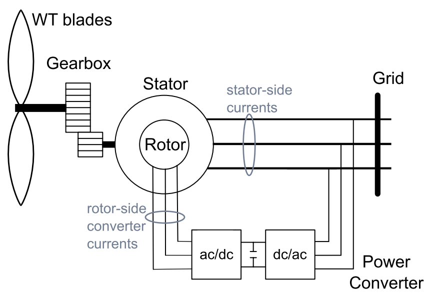

FIGURE 1. DFIG diagram indicating current measurements.

TABLE 1. Characteristics of the signals used for the analysis.

Current Transducer	Measurement type	Sampling Parameters
HOP 2000-SB/SP1 $\pm$3000 A	Stator-side current phase a Stator-side current phase b Stator-side current phase c Rotor-side converter current phase a Rotor-side converter current phase b Rotor-side converter current phase c	1.5 kHz 5.4 s

The DFIG was originally misdiagnosed with a bearing fault using root mean square (RMS) vibration analysis alone. Anomalous RMS levels were observed in the drive-end generator bearing, and the bearing was replaced. The RMS vibrations decreased slightly, but a few days later, the RMS vibrations rose to the level prior to the replacement. A healthy bearing was unnecessarily replaced and, thus, the actual fault continued. The chronological development of these events is presented in Figure 2.

A subsequent analysis of the current signals through CSA presented in [51] diagnosed the DFIG with rotor mechanical unbalance. This analysis was based on the presence of rotor mechanical related frequencies, these being f_{FRU} and f_{RFS}, calculated as Equations 8 and 9, respectively. The analysis is

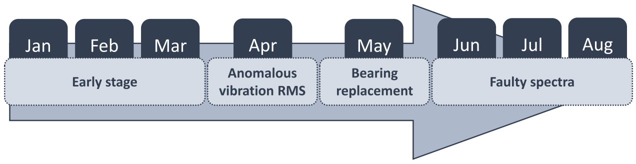

FIGURE 2. Chronological diagram of the DFIG under study.

summarized in Figure 3, showing the evolution of the current spectra from January to August, and Tables 2 and 3, indicating the fault frequencies observed in the spectra as previously reported.

$$f_{FRU} = f_s \left| \frac{\kappa}{p}(1-s) \pm 1 \right| \quad (8)$$

$$f_{RFS} = f_s \left(1 \pm 2\kappa s\right) \quad (9)$$

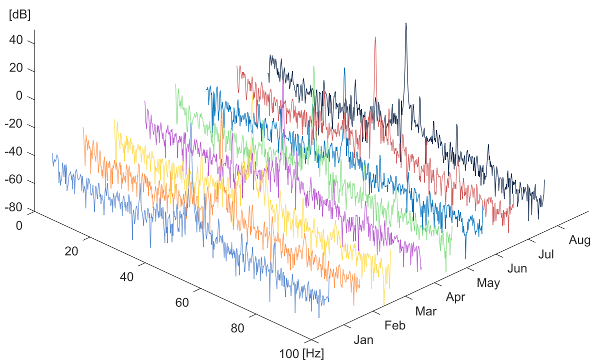

FIGURE 3. Evolution of current spectra Jan–Aug.

TABLE 2. Fault-related frequencies calculated as per equations 8 and 9, for -10% slip.

κ	f_{FRU} [Hz]	f_{RFS} [Hz]
-1	31.7	40.1
+1	68.3	59.9
-3		20.3
+3		79.7

TABLE 3. Fault-related frequency harmonics found on the current spectra from January 2016 to August 2016.

Month	f_{FRU}	f_{RFS}
Jan	±1	$\pm1, +3$
Feb	±1	$\pm1, +3$
Mar	±1	$\pm1, +3$
Apr	±1	$\pm1, \pm3$
May	±1	$\pm1, \pm3$
Jun	±1	$\pm1, +3$
Jul	±1	$\pm1, \pm3$
Aug	±1	$\pm1, \pm3$

The aim of the abovementioned previous work [51] was to achieve the correct diagnosis for the DFIG under study. However, it failed to analyze the behavior of the target fault. Thus, the goal of the present study is to observe the evolution of a developing fault over time. To this end, in order to make sure that the differences observed are caused by the target fault and are not due to any other cause, the measurements are chosen to meet steady-state conditions and the same (or very similar) loading conditions. The loading condition for each measurement is detailed in Table 4 and the criteria used to select steady-state regime signals is explained as follows:

TABLE 4. WT operating conditions for the selected measurements.

Month	Power [kW]	Speed Shaft [rpm]	Slip (per unit)
Jan	1081		
Feb	1094		
Mar	1100		
Apr	1100	1100	-10%
May	1100		
Jun	1098		
Jul	1087		
Aug	1086		

1) Each measurement is divided into eight parts. For each part:
   - The mains frequency of stator currents is calculated.
   - The mains frequency of rotor-side converter currents is calculated.
   - The RMS value of raw stator currents is calculated.
   - The RMS value of raw rotor-side converter currents is calculated.
2) Then, the following criteria must be met:
   - The mains frequencies of the stator currents remain constant.
   - The mains frequencies of rotor-side currents remain constant.
   - The differences between the RMS values of the stator and rotor-side currents are lower than 1.5%.

IV. RESULTS

In the present work, WSD is implemented to analyze the evolution of the current spectra of an in-service DFIG with an incipient fault. As presented in Section III, CSA proved to be successful in achieving the diagnosis of WT DFIGs. However, CSA alone failed to provide the quantitative and/or qualitative analysis of the evolution of a potentially developing fault. The interested reader can refer to the full study in [51], summarized in Section III, to understand the difficulty in comparing the various current spectra for the different months. Thus, in order to overcome this limitation, WSD is proposed.

As explained in Section II, WSD is able to estimate the similarities between two time series for different finite time and frequency intervals. This analysis is presented both qualitatively, using a graphical color scale, and quantitatively, analyzing the percentage of dissimilarities. Figures 4, 5 and 6 illustrate the qualitative results of applying

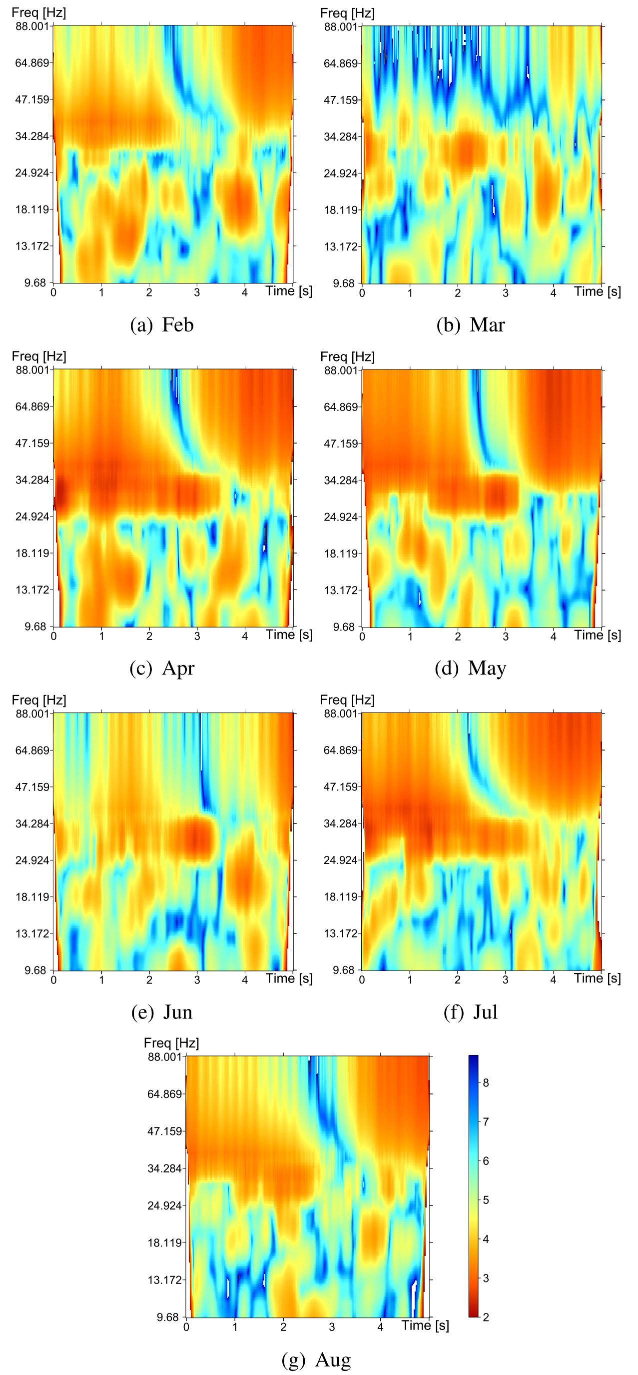

FIGURE 4. Phase a. Evolution of current spectra, comparing January with the next 7 months (Feb – Aug).

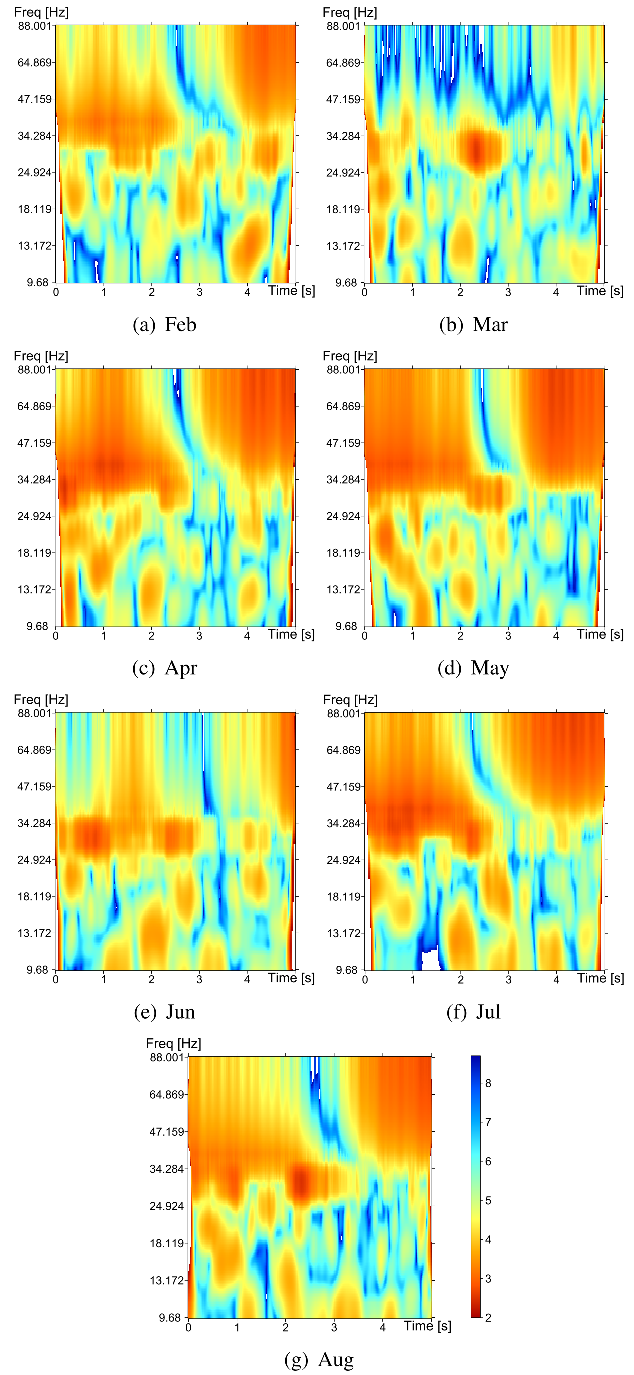

FIGURE 5. Phase b. Evolution of current spectra, comparing January with the next 7 months (Feb – Aug).

WSD to the stator current measurements (Phases a, b and c, respectively) of the DFIG under study. Then, the quantitative analysis is presented.

Regarding the qualitative analysis, since the objective of the present work was to estimate the divergence over time of the target frequencies (Table 2), as opposed to estimating the similarities as per the original algorithm, in the present color scale, red represents the highest dissimilarity and blue the highest similarity. To this end, January is taken as the reference, and each of the following months until August is compared to January. Figure 4(a) represents the divergence of the stator current spectra in February compared to that in January, Figure 4(b) represents the divergence between March and January, and so on up until Figure 4(g) representing the divergence between August and January. The same procedure was followed for the three stator current phases, a, b and c.

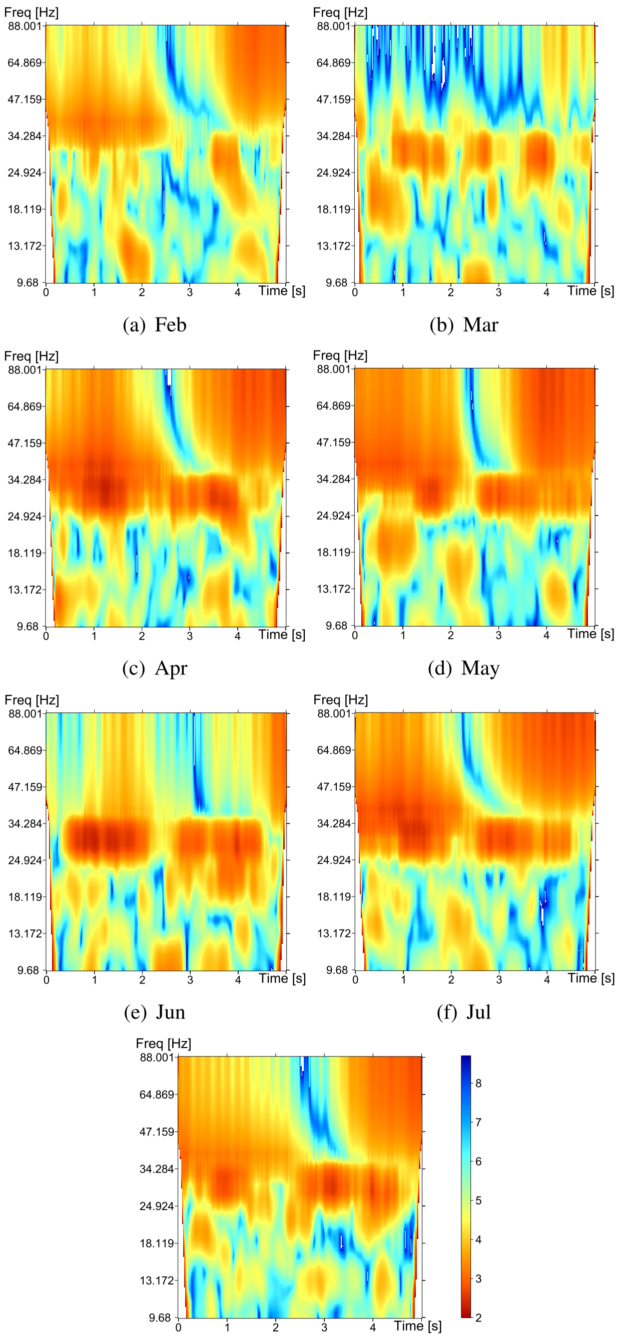

(a) Feb (b) Mar (c) Apr (d) May (e) Jun (f) Jul (g) Aug

FIGURE 6. Phase c. Evolution of current spectra, comparing January with the next 7 months (Feb – Aug).

As can be observed looking at each WSD individually, the largest dissimilarities (red bands) appear in the region of 30 Hz and 70 Hz, corresponding to f_{FRU}. Smaller, but still significant differences (red and orange spots), can be seen around 40 Hz and 60 Hz, and 20 Hz and 80 Hz, belonging to f_{RFS}. When looking at the WSDs as a whole for each month compared, a clear evolution of the fault from February to August cannot be determined. It appears that the comparisons obtained in April, May and July produce the largest differences, showing larger red areas. The lowest divergences are observed for the comparisons achieved for March and June, which agrees with Table 3, where fewer fault-related frequencies appear in those months. Note that all mentioned observations apply to all three phases (Figures 4, 5 and 6), i.e., no differences were observed between phases.

In order to quantify the results, the numerical values obtained from the raw WSD matrix around the frequencies of interest (the fault-related frequencies presented in Table 2) were averaged and the dissimilarity percentage was calculated. The results are shown in Figure 7. As can be seen, all frequencies of interest present a soft incremental tendency, except for component f_{RFS} with $\kappa = -3$. The largest differences are obtained for April, May and July, and the lowest for March and June, thus confirming the conclusions drawn from the graphical analysis.

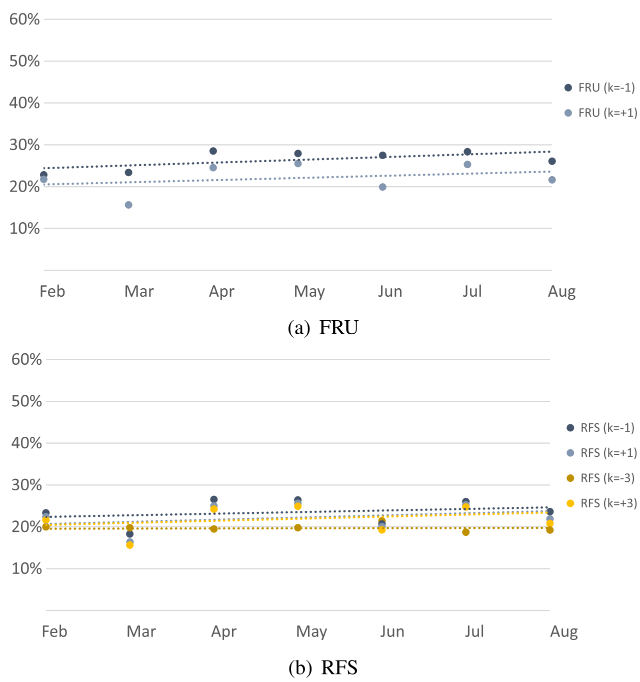

(a) FRU (b) RFS

FIGURE 7. WSD percentage variation of fault related frequencies.

V. CONCLUSION

With the objective of optimizing O&M costs towards reducing the LCOE of wind energy, the present paper introduces an innovative CM wavelet-based method applied to an in-service WT generator, which is one of the most critical components regarding the availability and reliability of WTs.

The machine under study had been previously diagnosed with rotor mechanical unbalance using CSA, validated with advanced vibration analysis. This study, however, failed to investigate the evolution of the fault over the period explored.

In the present study, for the first time in the scientific literature, WSD was implemented to the stator currents of a WT DFIG operating in the field, in contrast to the majority of the published studies, which are based on laboratory benches or computer simulations. WSD is a novel wavelet-based technique able to estimate the similarities between two time series in the time-frequency domain. This technique allowed us to compare the fault-related frequencies present in the stator current signals, the dissimilarities in this case, thus allowing the evolution of the previously diagnosed fault to be tracked and quantified. The results of the analysis were presented graphically comparing the reference month (January) to each of the following months until August, as well as quantitatively analyzing the percentage of dissimilarities. Both the graphical and the quantitative analyses proved to be successful in tracking the target (fault-related) frequencies.

In conclusion, CSA is able to identify the fault, however, it is limited to quantify and track its evolution. On the other hand, whilst WSD is able to overcome this limitation, the method alone is not able to achieve the diagnosis. Thus, the combination of CSA (able to achieve a diagnosis) and WSD (able to track and quantify the evolution of the fault) shows strong potential in developing CM for WTs. In this regard, predictive maintenance techniques based on CM are applied individually to each WT in the wind farm, such as commercial CM systems based on oil analysis, SCADA and/or vibration data. The analysis of the current spectra proposed towards monitoring the induction generator is also performed individually and, therefore, it can be easily applied to any WT fleet size, following the same procedure that the mentioned commercial systems.

REFERENCES

[1] *Kyoto Protocol to the United Nations Framework Convetion on Climate Change*, United Nations, New York, NY, USA, 1998.

[2] *A European Strategic Energy Technology Plan (SET-Plan)—Towards a Low Carbon Future*, Commission Eur. Communities, Brussels, Belgium, 2007.

[3] A. Honrubia-Escribano, E. Gómez-Lázaro, J. Fortmann, P. Sørensen, and S. Martin-Martinez, "Generic dynamic wind turbine models for power system stability analysis: A comprehensive review," *Renew. Sustain. Energy Rev.*, vol. 81, pp. 1939–1952, Jan. 2018.

[4] F. Z. J. Lee, "Global wind report 2021," Global Wind Energy Council, Brussels, Belgium, Tech. Rep., 2021.

[5] D. Gielen, R. Gorini, N. Wagner, R. Leme, G. Prakash, R. Ferroukhi, M. Renner, B. Parajuli, and X. G. Casals, "Global renewables outlook: Energy transformation 2050," Int. Renew. Energy Agency, Abu Dhabi, United Arab Emirates, Tech. Rep., 2020.

[6] F. P. G. Márquez, A. M. Tobias, J. M. P. Pérez, and M. Papaelias, "Condition monitoring of wind turbines: Techniques and methods," *Renew. Energy*, vol. 46, pp. 169–178, Oct. 2012.

[7] J. Carroll, A. McDonald, and D. Mcmillan, "Failure rate, repair time and unscheduled O&M cost analysis of offshore wind turbines," *Wind Energy*, vol. 19, no. 6, pp. 1107–1119, Jun. 2016.

[8] F. P. G. Márquez, J. M. P. Pérez, A. P. Marugán, and M. Papaelias, "Identification of critical components of wind turbines using FTA over the time," *Renew. Energy*, vol. 87, pp. 869–883, Mar. 2016.

[9] E. Artigao, S. Martín-Martínez, A. Honrubia-Escribano, and E. Gómez-Lázaro, "Wind turbine reliability: A comprehensive review towards effective condition monitoring development," *Appl. Energy*, vol. 228, pp. 1569–1583, Oct. 2018.

[10] M. F. El-Naggar, A. S. Abdelhamid, M. A. Elshahed, and M. El-Shimy Mahmoud Bekhet, "Ranking subassemblies of wind energy conversion systems concerning their impact on the overall reliability," *IEEE Access*, vol. 9, pp. 53754–53768, 2021.

[11] R. A. J. Amalorpavaraj, P. Kaliannan, S. Padmanaban, U. Subramaniam, and V. K. Ramachandaramurthy, "Improved fault ride through capability in DFIG based wind turbines using dynamic voltage restorer with combined feed-forward and feed-back control," *IEEE Access*, vol. 5, pp. 20494–20503, 2017.

[12] N. Ullah, M. A. Ali, A. Ibeas, and J. Herrera, "Adaptive fractional order terminal sliding mode control of a doubly fed induction generator-based wind energy system," *IEEE Access*, vol. 5, pp. 21368–21381, 2017.

[13] K. Brigham, D. Zappalá, C. J. Crabtree, and C. Donaghy-Spargo, "Simplified automatic fault detection in wind turbine induction generators," *Wind Energy*, vol. 23, no. 4, pp. 1135–1144, Apr. 2020.

[14] X. Jin, Z. Xu, and W. Qiao, "Condition monitoring of wind turbine generators using SCADA data analysis," *IEEE Trans. Sustain. Energy*, vol. 12, no. 1, pp. 202–210, Jan. 2021.

[15] A. Turnbull, J. Carroll, and A. McDonald, "Combining SCADA and vibration data into a single anomaly detection model to predict wind turbine component failure," *Wind Energy*, vol. 24, no. 3, pp. 197–211, Mar. 2021.

[16] E. Artigao, A. Honrubia-Escribano, and E. Gomez-Lazaro, "Current signature analysis to monitor DFIG wind turbine generators: A case study," *Renew. Energy*, vol. 116, pp. 5–14, Feb. 2018.

[17] D. Zappalá, N. Sarma, S. Djurović, C. J. Crabtree, A. Mohammad, and P. J. Tavner, "Electrical & mechanical diagnostic indicators of wind turbine induction generator rotor faults," *Renew. Energy*, vol. 131, pp. 14–24, Feb. 2019.

[18] W. Touti, M. Salah, K. Bacha, Y. Amirat, A. Chaari, and M. Benbouzid, "An improved electromechanical spectral signature for monitoring gear-based systems driven by an induction machine," *Appl. Acoust.*, vol. 141, pp. 198–207, Dec. 2018.

[19] Y. Gritli, L. Zarri, C. Rossi, F. Filippetti, G.-A. Capolino, and D. Casadei, "Advanced diagnosis of electrical faults in wound-rotor induction machines," *IEEE Trans. Ind. Electron.*, vol. 60, no. 9, pp. 4012–4024, Sep. 2013.

[20] P. J. Tavner, "Review of condition monitoring of rotating electrical machines," *IET Electr. Power Appl.*, vol. 2, no. 4, pp. 215–247, Jul. 2008.

[21] M. El H. Benbouzid, "A review of induction motors signature analysis as a medium for faults detection," *IEEE Trans. Ind. Electron.*, vol. 47, no. 5, pp. 984–993, Oct. 2000.

[22] A. Siddique, G. S. Yadava, and B. Singh, "A review of stator fault monitoring techniques of induction motors," *IEEE Trans. Energy Convers.*, vol. 20, no. 1, pp. 106–114, Mar. 2005.

[23] M. E. H. Benbouzid and G. B. Kliman, "What stator current processing-based technique to use for induction motor rotor faults diagnosis?" *IEEE Trans. Energy Convers.*, vol. 18, no. 2, pp. 238–244, Jun. 2003.

[24] W. Qiao and L. Qu, "Prognostic condition monitoring for wind turbine drivetrains via generator current analysis," *Chinese J. Electr. Eng.*, vol. 4, no. 3, pp. 80–89, 2018.

[25] S. Djurovic, C. J. Crabtree, P. J. Tavner, and A. Smith, "Condition monitoring of wind turbine induction generators with rotor electrical asymmetry," *IET Renew. Power Gener.*, vol. 6, no. 4, pp. 207–216, 2012.

[26] R. K. Ibrahim, S. J. Watson, S. Djurovic, and C. J. Crabtree, "An effective approach for rotor electrical asymmetry detection in wind turbine DFIGs," *IEEE Trans. Ind. Electron.*, vol. 65, no. 11, pp. 8872–8881, Nov. 2018.

[27] Y. Amirat, V. Choqueuse, M. Benbouzid, and J.-F. Charpentier, "Bearing fault detection in DFIG-based wind turbines using the first intrinsic mode function," in *Proc. 19th Int. Conf. Electr. Mach. (ICEM)*, 2010, pp. 1–6.

[28] Q. F. Lu, Z. T. Cao, and E. Ritchie, "Model of stator inter-turn short circuit fault in doubly-fed induction generators for wind turbine," in *Proc. IEEE 35th Annu. Power Electron. Specialists Conf.*, Jun. 2004, pp. 932–937.

[29] S. Djurovic, S. Williamson, and A. Renfrew, "Dynamic model for doubly-fed induction generators with unbalanced excitation, both with and without winding faults," *IET Electr. Power Appl.*, vol. 3, no. 3, pp. 171–177, 2009.

[30] R. J. Romero-Troncoso, R. Saucedo-Gallaga, E. Cabal-Yepez, A. Garcia-Perez, R. A. Osornio-Rios, R. Alvarez-Salas, H. Miranda-Vidales, and N. Huber, "FPGA-based online detection of multiple combined faults in induction motors through information entropy and fuzzy inference," *IEEE Trans. Ind. Electron.*, vol. 58, no. 11, pp. 5263–5270, Nov. 2011.

[31] S. H. Kia, H. Henao, and G.-A. Capolino, "Gear tooth surface damage fault detection using induction machine electrical signature analysis," in *Proc. 9th IEEE Int. Symp. Diagnostics Electr. Mach., Power Electron. Drives (SDEMPED)*, Aug. 2013, pp. 358–364.

[32] S. H. Kia, H. Henao, and G.-A. Capolino, "Fault index statistical study for gear fault detection using stator current space vector analysis," *IEEE Trans. Ind. Appl.*, vol. 52, no. 6, pp. 4781–4788, Nov. 2016.

[33] F. Cheng, L. Qu, and W. Qiao, "Fault prognosis and remaining useful life prediction of wind turbine gearboxes using current signal analysis," *IEEE Trans. Sustain. Energy*, vol. 9, no. 1, pp. 157–167, Jan. 2018.

[34] S. Choi, B. Akin, M. M. Rahimian, and H. A. Toliyat, "Implementation of a fault-diagnosis algorithm for induction machines based on advanced digital-signal-processing techniques," *IEEE Trans. Ind. Electron.*, vol. 58, no. 3, pp. 937–948, Mar. 2011.
[35] S. Choi, B. Akin, M. M. Rahimian, and H. A. Toliyat, "Performance-oriented electric motors diagnostics in modern energy conversion systems," *IEEE Trans. Ind. Electron.*, vol. 59, no. 2, pp. 1266–1277, Feb. 2012.
[36] M. R. Shahriar, P. Borghesani, and A. C. C. Tan, "Electrical signature analysis-based detection of external bearing faults in electromechanical drivetrains," *IEEE Trans. Ind. Electron.*, vol. 65, no. 7, pp. 5941–5950, Jul. 2018.
[37] Y. Qin, J. Zou, and F. Cao, "Adaptively detecting the transient feature of faulty wind turbine planetary gearboxes by the improved kurtosis and iterative thresholding algorithm," *IEEE Access*, vol. 6, pp. 14602–14612, 2018.
[38] P. Zhang and P. Neti, "Detection of gearbox bearing defects using electrical signature analysis for doubly-fed wind generators," in *Proc. IEEE Energy Convers. Congr. Expo.*, Sep. 2013, pp. 4438–4444.
[39] F. Cheng, L. Qu, W. Qiao, C. Wei, and L. Hao, "Fault diagnosis of wind turbine gearboxes based on DFIG stator current envelope analysis," *IEEE Trans. Sustain. Energy*, vol. 10, no. 3, pp. 1044–1053, Jul. 2019.
[40] O. Rioul and M. Vetterli, "Wavelets and signal processing," *IEEE Signal Process. Mag.*, vol. 8, no. 4, pp. 14–38, Oct. 1991.
[41] V. J. Bolós, R. Benítez, R. Ferrer, and R. Jammazi, "The windowed scalogram difference: A novel wavelet tool for comparing time series," *Appl. Math. Comput.*, vol. 312, pp. 49–65, Nov. 2017.
[42] K. C. Raath and K. B. Ensor, "Time-varying wavelet-based applications for evaluating the water-energy nexus," *Frontiers Energy Res.*, vol. 8, p. 118, Jun. 2020.
[43] V. J. Bolós and R. Benítez, *The Wavelet Scalogram in the Study of Time Series*. Cham, Switzerland: Springer, 2014, pp. 147–154.
[44] D. Zhang, *Wavelet Transform*. Cham, Switzerland: Springer, 2019, pp. 35–44.
[45] H. Boubaker and H. Rezgui, "Co–movement between some commodities and the Dow Jones Islamic index: A wavelet analysis," *Econ. Bull.*, vol. 40, no. 1, pp. 574–586, 2020.
[46] Y.-G. Yang, P. Xu, R. Yang, Y.-H. Zhou, and W.-M. Shi, "Quantum hash function and its application to privacy amplification in quantum key distribution, pseudo-random number generation and image encryption," *Sci. Rep.*, vol. 6, no. 1, p. 19788, Apr. 2016.
[47] S. Behnia, J. Ziaei, M. Ghiassi, and M. Yahyavi, "Comprehensive chaotic description of heartbeat dynamics using scale index and Lyapunov exponent," *Omega*, vol. 500, pp. 1–5, Jun. 2013.
[48] Q. Fan, Y. Wang, and L. Zhu, "Complexity analysis of spatial–temporal precipitation system by PCA and SDLE," *Appl. Math. Model.*, vol. 37, no. 6, pp. 4059–4066, Mar. 2013.
[49] V. Piccirillo, J. M. Balthazar, A. M. Tusset, D. Bernardini, and G. Rega, "Characterizing the nonlinear behavior of a pseudoelastic oscillator via the wavelet transform," *Proc. Inst. Mech. Eng., C, J. Mech. Eng. Sci.*, vol. 230, no. 1, pp. 120–132, Jan. 2016.
[50] J. L. P. Felix, J. M. Balthazar, Â. M. Tusset, V. Piccirillo, A. M. Bueno, and R. M. L. R. da Fonseca, "On optimal control of a nonlinear robotic mechanism using the saturation phenomenon," in *Structural Nonlinear Dynamics and Diagnosis*. Cham, Switzerland: Springer, 2015, pp. 145–165.
[51] E. Artigao, S. Koukoura, A. Honrubia-Escribano, J. Carroll, A. McDonald, and E. Gómez-Lázaro, "Current signature and vibration analyses to diagnose an in-service wind turbine drive train," *Energies*, vol. 11, no. 4, p. 960, Apr. 2018.

ESTEFANIA ARTIGAO received the M.Sc. and Ph.D. degrees in industrial engineering from the University of Castilla-La Mancha (UCLM), Spain, in 2009 and 2018, respectively, where she is currently pursuing the Ph.D. degree. Since 2010, she has been working with several research entities at U.K., including the University of Birmingham, Birmingham; TWI Ltd., Cambridge; and Brunel University London, London, where she worked on research and development projects within the wind energy sector. In July 2015, she received the Marie Curie ITN Grant under the H2020 Program to carry out her Ph.D. studies at UCLM, where she is currently a Research Fellow. Her main research interests include operation and maintenance and condition monitoring of wind turbines.

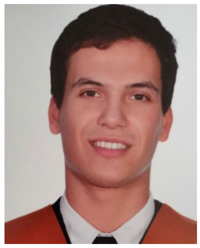

JOSÉ MIGUEL BALLESTER-ARCE received the B.Sc. degree (Hons.) in industrial engineering from the Universidad Politécnica de Cartagena (UPCT), in 2020, where he is currently pursuing the M.Sc. degree in industrial engineering. In September 2020, he was awarded the Fellowship "Energy analysis and management, and environmental regulations" and gained a placement at Estrella de Levante, Murcia, Spain, where he works on renewable energy projects with the Environment and Energy Optimization Department, combined with his M.Sc. studies.

MARÍA CARMEN BUESO received the B.Sc. and Ph.D. degrees in mathematics from the Universidad de Granada, Spain, in 1992 and 1996, respectively. She is currently an Associate Professor with the Department of Applied Mathematics and Statistics, Universidad Politécnica de Cartagena, Spain. Her research interests include space-temporal modeling of stochastic processes, derivation of related inference procedures and sampling strategies, and statistical analysis, modeling, and inference of physic-chemical and environmental processes.

ANGEL MOLINA-GARCÍA (Senior Member, IEEE) received the degree in electrical engineering from the Universidad Politécnica de Valencia, Valencia, Spain, in 1998, and the Ph.D. degree in electrical engineering from the Universidad Politécnica de Cartagena, Cartagena, Spain, in 2003. He is currently a Professor with the Department of Automatics, Electrical Engineering and Electronic Technology, Universidad Politécnica de Cartagena. His research interests include wind power generation, PV power plants, energy efficiency, and demand response.

ANDRÉS HONRUBIA ESCRIBANO received the degree in electrical engineering from the Polytechnic University of Madrid (UPM), Madrid, Spain, in 2008, and the Ph.D. degree in renewable energy from the Polytechnic University of Cartagena, Cartagena, Spain, in 2012. Since 2008, he has been working with several research entities, publishing more than 100 articles in journals, books, specialized conferences, and collaborating in more than 60 research and development projects. He is currently an Associate Professor with the Department of Electrical, Electronics, and Control Engineering, University of Castilla-La Mancha, Albacete, Spain. His main research interest includes the integration of wind energy into power systems.

EMILIO GÓMEZ LÁZARO (Senior Member, IEEE) received the M.Sc. and Ph.D. degrees in electrical engineering from the Universidad Politecnica de Valencia, Valencia, Spain, in 1995 and 2000, respectively. He is currently a Full Professor with the Department of Electrical, Electronics, and Control Engineering, University of Castilla-La Mancha, Albacete, Spain, where he is also the Director of the Renewable Energy Research Institute. His research interests include modeling of wind turbines and wind farms, grid codes, power system integration studies, steady-state and dynamic analysis, and maintenance of renewable energy power plants.